

# Curcumin nanoparticles combined with narlumosbart regulate wingless-type MMTV integration site (wnt)/ $\beta$ -catenin signaling pathway in osteoblast-like cells

Heng Zhang and Yonggang Zhao\*

Department of Orthopaedic Surgery (hand and foot trauma), People's Hospital of Dongxihu, Wuhan, Hubei, China

**Abstract:** **Background:** Narlumosbart is a key agent for modulating bone cell function. Given the potential of curcumin nanoparticles to inhibit cell growth when applied alone. **Objectives:** This study aims to investigate the role of their combination with narlumosbart in bone trauma repair and cell cycle regulation. **Methods:** Curcumin nanoparticles were fabricated and applied in combination with narlumosbart to treat MC3T3-E1 cells. The effects of this combination on osteoblast differentiation and proliferation were then assessed through immunofluorescence, protein expression analysis and ALP activity assays. **Results:** The combined use of curcumin nanoparticles and narlumosbart at 4  $\mu$ M significantly enhanced inhibitory activity, indicating a synergistic therapeutic effect. Furthermore, immunohistochemistry revealed a marked increase in  $\beta$ -catenin expression and activation of the Wnt/ $\beta$ -catenin signaling pathway in the combination group. In contrast, while ALP staining confirmed elevated ALP activity, immunofluorescence detection showed no significant change in cell proliferation. **Conclusion:** Loaded within narlumosbart, curcumin nanoparticles can precisely modulate the Wnt/ $\beta$ -catenin pathway. This process specifically induces osteogenic differentiation without impacting proliferation, thereby directing cellular processes towards bone formation.

**Keywords:** Bone trauma; Curcumin nanoparticles; Narlumosbart; Wnt/B-catenin

*Submitted on 22-09-2025 – Revised on 15-12-2025 – Accepted on 24-12-2025*

## INTRODUCTION

Bone trauma is the most common skeletal system disease (Collaborators, 2021, Seitz *et al.*, 2008). Traditional drugs have poor efficacy. This year, new drugs developed have better efficacy. narlumosbart was developed by Shanghai Jinmante Biotechnology Co., Ltd. and is a novel fully human monoclonal antibody with a hinge region containing two disulfide bonds and a mutation to S228P that prevents Fab arm exchange, making the conformation uniform and the structure stable (Coupaud *et al.*, 2015, Mitchell *et al.*, 2018). In addition, narlumosbart has a stronger affinity for RANKL, but its clinical application is limited due to its fast metabolic rate, low osteosarcoma affinity, high cardiotoxicity, bone marrow suppression and other side effects (Wan *et al.*, 2021, Wang *et al.*, 2020). How to improve the *in-vivo* enrichment of narlumosbart and improve patient prognosis is still an urgent problem in the current clinical treatment of bone trauma.

In recent years, researchers have developed a variety of nano-drug delivery systems to improve the clinical efficacy of drugs in bone trauma, including bisphosphonates, hyaluronic acid, folic acid, polydopamine, peptides, etc. However, such synthetic drugs often cannot specifically bind to bone cells (Niu *et al.*, 2023, Tomlinson *et al.*, 2017). A single administration of polydopamine has little effect on cell growth because the penetration of polydopamine into cells is limited and the cells are hypoxic, so the amount

of polydopamine produced is limited. Therefore, many studies focus on creating a penetrable hypoxic intracellular microenvironment to enhance the toxicity of hypoxia-sensitive prodrugs. The polymer has a small particle size (33nm) and high stability. Strong and controllable drug release (Azeem *et al.*, 2012). In a non-redox environment, the amount of drug released from the polymer is less than 10%, but under glutathione stimulation, about 86% of the total drug can be released in 12 hours (Chen *et al.*, 2018).

Curcumin-based nanoparticles (NPs) are non-toxic and non-immunogenic, making them a promising drug carrier. Curcumin-based NPs can be loaded with other chemotherapy drugs and inhibitors for targeted delivery to reduce side effects and have been used in various fields such as electroacoustic devices, lubrication, carbon nanotubes and antibacterial and deodorizing plastics (Liu *et al.*, 2020, Zhu *et al.*, 2023). Using curcumin nanoparticles as carriers, the stability and water solubility of narlumosbart were significantly improved.

In mesenchymal stem cells, low pH is critical in cell progression (Chao *et al.*, 2020, Zhuang *et al.*, 2023) and behaviors (Dai *et al.*, 2019, Richbourg *et al.*, 2020). Specifically, low pH activates the wnt/ $\beta$ -catenin pathway in MSCs, thereby activating the transcription of  $\beta$ -catenin (Richbourg *et al.*, 2020, Zhuang *et al.*, 2023). Curcumin is a natural compound extracted from the rhizome of *Curcuma longa* L., and widely applied in several aspects (Wei *et al.*, 2019). Curcumin inhibits  $\beta$ -catenin

\*Corresponding author: e-mail: jiluanxinf@126.com

translocation into the nucleus (Antoon *et al.*, 2013). Therefore, it can prevent the transcription of downstream pro-inflammatory proteins to exert anti-inflammatory (Rishabh *et al.*, 2021) and anti-cancer (Zhu *et al.*, 2018) activities.

Although people are increasingly interested in the anti-cancer effects of curcumin, curcumin currently has poor stability, solubility and oral bioavailability, which limits its application. Encapsulation of curcumin is expected to enhance its antioxidant activity. In this study, the therapeutic value of curcumin nanoparticles in osteoblast-like cells was assessed as a foundation for future *in-vivo* studies.

## MATERIALS AND METHODS

### *Synthesis and preparation of curcumin nanoparticles*

Curcumin nanoparticles were synthesized using the nanoprecipitation method. Curcumin (10 mg) and PLGA (50 mg) were dissolved in acetone (5 mL), then slowly dripped into an aqueous phase containing 1% PVA. The mixture was stirred overnight and nanoparticles were collected by centrifugation and washed three times with deionized water. The resulting nanoparticles can be used for *in-vivo* injection or can be used in the next step to prepare TDPA-coated nanoparticles *in-vitro*. The mean size and electrokinetic potential were measured using dynamic laser scattering (DLS) and a Zetasizer 3000 HS particle analyzer (Malvern Instruments Ltd, Worcester, UK). Size and zeta potential values are expressed as the average of three measurements. The molecular formula of curcumin nanoparticles is shown in fig. 1A.

### *In vitro drug release study*

The *in vitro* release profile of curcumin from nanoparticles was evaluated using the dialysis bag method. Briefly, 2 mg of freeze-dried curcumin nanoparticles were suspended in 2 mL of phosphate-buffered saline (PBS) at pH 5, 6.8, and 7.4, respectively, and placed into a dialysis bag (molecular weight cutoff: 3.5 kDa). The bag was immersed in 30 mL of the corresponding release medium and incubated at 37 °C with gentle shaking (100 rpm). At predetermined time intervals (0, 2, 4, 6, 8, 24, 48, and 72 h), 1 mL of the external medium was withdrawn and replaced with an equal volume of fresh medium. The concentration of curcumin released was measured using a UV-Vis spectrophotometer at 425 nm. All experiments were performed in triplicate, and the cumulative release percentage was calculated and plotted against time.

### *Cell culture*

Mouse embryonic osteoblast precursor cells MC3T3-E1 (Biomax); Primary antibody (P65, 1:1000; GAPDH, 1:1000) (Abcam Company); secondary antibody (Santa Cruz Company); fetal calf Serum, Penicillin and Streptomycin (Costar Company); LipofectamineTM2000

kit, Flow cytometer, Electrophoresis tank (Merck Company); Transmission electron microscope, Particle analyzer (Zhuhai O&M). The *in-vitro* experiments conducted in this study adhered to the institutional ethical guidelines governing the overall research project. This paper reports the preclinical cytological findings from this research series, providing a theoretical basis and dosage references for future *in-vivo* experiments.

### *ELISA*

The cell supernatant was collected and the absorbance value at 450nm wavelength was measured by Enzymoscope according to the operation method of IL-6 and IL-8 kit (Shanghai Gudou Biotechnology, 1:100) and the concentration of IL-6 and IL-8 was calculated after the standard curve was drawn.

### *Immunofluorescence*

The cells were washed after fixation, blocked after permeabilization and then blocked for 60 min (Im *et al.*, 2019). The cells were then diluted 1:200 with primary antibodies overnight and with secondary antibodies for 1 hour. After washing with PBS, added DAPI for 5 min and took images.

### *Western blot*

Protein was lysed using RIPA buffer (Shanghai Sangon Biotechnology Co., Ltd.) and incubated overnight at 4 °C with a 1:1000 primary antibody prepared by buffer (Shanghai Sangon Biotechnology Co., Ltd.). GAPDH antibody (CST Biological Co., Ltd., USA) was used as the internal reference. After washing, incubate the membrane with the secondary antibody for 1 hour at room temperature and perform imaging after 24 hours.

### *Cell proliferation*

Cell Counting Kit-8 (CCK-8; Shanghai Sangon Biotechnology Co., Ltd.) was used (Fan *et al.*, 2024). Osteoblast precursor cell lines were distributed into 96-well plates ( $1 \times 10^5$  cells/200  $\mu$ l). The cells were treated with recombinant  $\beta$ -catenin protein at concentrations of 0, 0.1 and 0.5  $\mu$ g/mL, respectively. Subsequently, cell proliferation activity was measured at designated time points using the CCK-8 assay.

### *Statistical analysis*

SPSS® 20.0 and GraphPad Prism16.0 were used for statistical analysis. The calculated data were expressed as (mean  $\pm$ SD). All data sets were confirmed to follow a normal distribution by the Shapiro-Wilk test. Comparisons between two groups were performed using an independent samples t-test. For comparisons across multiple groups, one-way analysis of variance (ANOVA) was employed. Considering the exploratory nature of the research design and equal sample sizes, Fisher's LSD test was selected for post-hoc multiple comparisons. Statistical significance was

defined as  $P < 0.05$ . All experiments were independently repeated three times with three replicate wells per group.

## RESULTS

### *Synthesis and characterization of curcumin nanoparticles*

Curcumin nanoparticles are generated through electrostatic interactions between positively charged cationic NPs and negatively charged surface polymers. Electron microscopy showed the presence of nanoparticles in the cytoplasm with an average size of  $(179 \pm 0.5)$  nm (Fig. 1B). In addition, under different PH environments, the 70 h *in-vitro* release of curcumin nanoparticles was lower than 85% (Fig. 1C), indicating that the synthesized curcumin nanoparticles in this study possess a desirable sustained-release property. Curcumin nanoparticles were prepared and displayed by scanning electron microscopy (Fig. 1D).

### *Anti-inflammatory activity of curcumin nanoparticles combined with narlumosbart*

Cells were exposed to a culture medium containing 4  $\mu$ M curcumin nanoparticles and a corresponding molar equivalent of narlumosbart. PBS was used as a control to ensure that the vehicle itself was not producing an effect. Curcumin nanoparticles loaded into narlumosbart showed a higher anti-inflammatory effect than free curcumin and narlumosbart alone, as the inhibitory activity was already significant at 4  $\mu$ M (Fig. 2, against IL-6 and  $p = 0.0090$  for IL8), indicating that loading of curcumin nanoparticles into narlumosbart improved its efficacy. PBS had no obvious effect on IL-6 secretion (Fig. 2A, 2B). This suggests that, compared with free curcumin or narlumosbart alone, the combined application of curcumin nanoparticles and narlumosbart significantly promoted the secretion of the inflammatory cytokines IL-6 and IL-8. This indicates that the combination may modulate the bone trauma microenvironment by activating specific immune or stress signaling pathways.

### *Wnt/ $\beta$ -catenin signaling is the direct target gene of curcumin nanoparticles combined with narlumosbart*

$\beta$ -catenin expression was higher in the curcumin nanoparticles combined with narlumosbart treatment group, as shown in Fig. 3A. The immunofluorescence results showed that the wnt/ $\beta$ -catenin signal was obvious in curcumin nanoparticles combined with narlumosbart treatment group (Fig. 3B). Higher than that in the narlumosbart treatment group. To further validate the changes in the Wnt/ $\beta$ -catenin pathway, the expression levels of the key signaling protein  $\beta$ -catenin and its downstream target c-Myc were assessed by Western blot. As shown in Fig. 3C, the protein expression of both  $\beta$ -catenin and c-Myc was significantly upregulated in the combination treatment group compared with either free curcumin nanoparticles or narlumosbart alone. Statistical analysis of the band grayscale values (Fig. 3D) confirmed

that this upregulation was statistically significant ( $P < 0.01$ ), indicating that the combination treatment synergistically activates the Wnt/ $\beta$ -catenin signaling pathway.

### *Effect of Wnt/ $\beta$ -catenin on osteogenesis and maintenance of bone homeostasis*

As seen in fig. 4A, the addition of the signaling pathway enhanced the staining of ALP. ALP staining results were similar, indicating that  $\beta$ -catenin significantly promoted the osteogenic activity of bone cells. Cell proliferation showed no differences between groups after exposure to 0.1, 0.5, or 1  $\mu$ g/mL  $\beta$ -catenin for 24 or 48 hours (Fig. 4B). Ki67 immunofluorescence staining detected the proliferation ability of  $\beta$ -catenin-stimulated osteocytes and the results showed no difference in proliferation (Fig. 4C, 4D). Therefore,  $\beta$ -catenin cannot promote bone cell proliferation.

## DISCUSSION

During bone development, Wnt/ $\beta$ -catenin signaling plays a key role in cell differentiation and bone matrix formation (Wu *et al.*, 2019). The imbalance between bone formation and resorption is critical for osteopenia and changes in bone structure (Mai *et al.*, 2024). Several studies indicate the role of Wnt/ $\beta$ -catenin signaling in osteoblastogenesis (Shi *et al.*, 2024). Wnt signaling pathway function in osteocytes, which are often used as bone models (Li *et al.*, 2021).

Nalusumab is the world's first fully human anti-RANKL monoclonal antibody of the IgG4 subtype approved for marketing. The currently marketed drug denosumab with the same target is of the IgG2 subtype. Compared with denosumab, its uniformity and quality controllability have been significantly improved (Li *et al.*, 2021).

This study mainly explores the effect and mechanism of curcumin nanoparticles + narlumosbart on the proliferation and cell cycle of rat bone trauma cells. In this study, curcumin nanoparticles were successfully prepared to interfere with bone cells. Previous studies have shown that curcumin nanoparticles activate the Wnt/ $\beta$ -catenin complex (Lv *et al.*, 2017). It was then verified whether curcumin nanoparticles + narlumosbart effectively damaged acid-induced bone cells. The secretion of inflammatory cytokines mediated by curcumin nanoparticles + narlumosbart was also assessed. It was observed that the combination treatment modulated inflammatory cytokine secretion, leading to increased levels of IL-6 and IL-8 compared with the control group. This alteration may be associated with the activation of early signaling events required for bone healing.

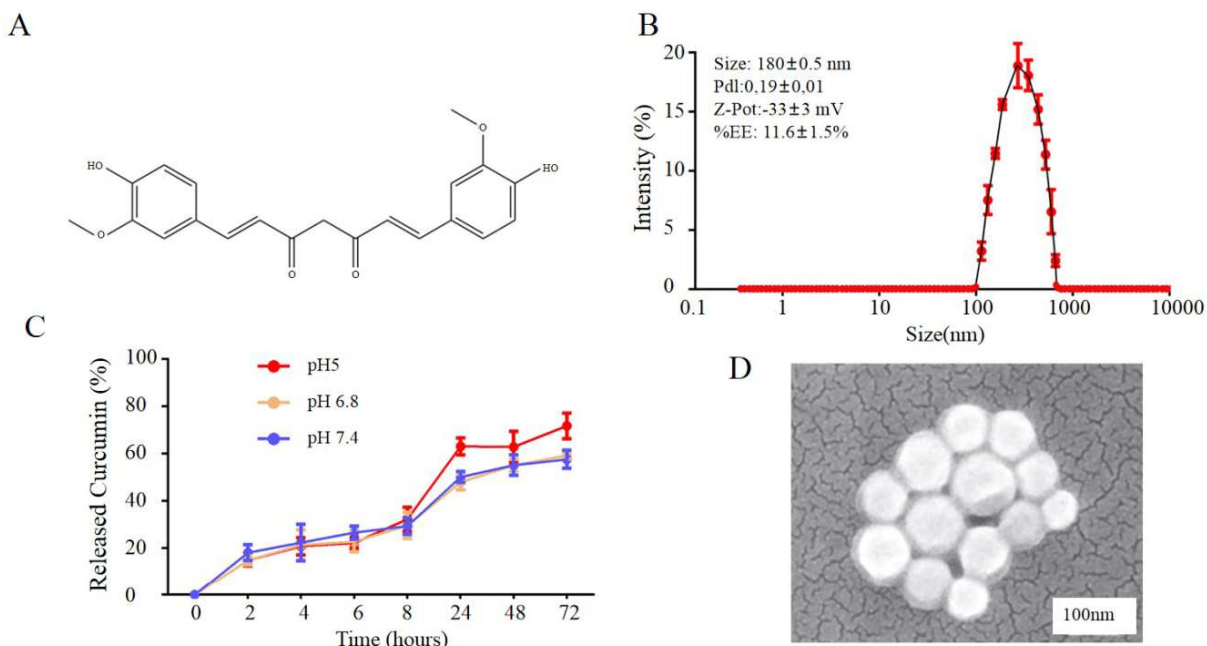


**Fig. 1:** Synthesis and characterization of curcumin nanoparticles. (A) Chemical structure of curcumin; (B) The size of curcumin nanoparticles; (C) Release curves of curcumin nanoparticles at different PH; (D) The surface morphology under a scanning electron microscope (The scale in the picture is 1:400).

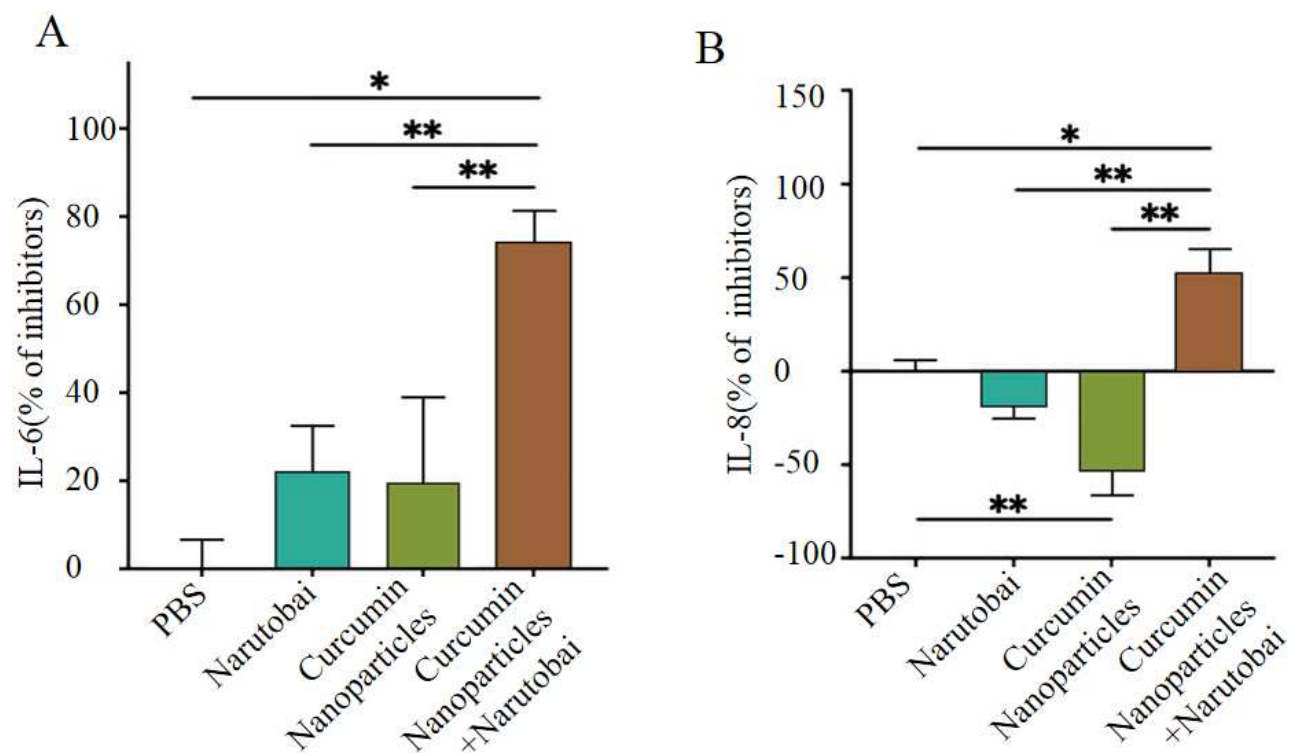


**Fig. 2:** Anti-inflammatory activity of curcumin nanoparticles combined with narlutobai. (A) IL-6 activity detection; (B) IL-8 activity detection. (\* means  $P < 0.05$ , \*\* means  $P < 0.01$ ). Y-axis indicates the inhibition of IL-6 or IL-8.

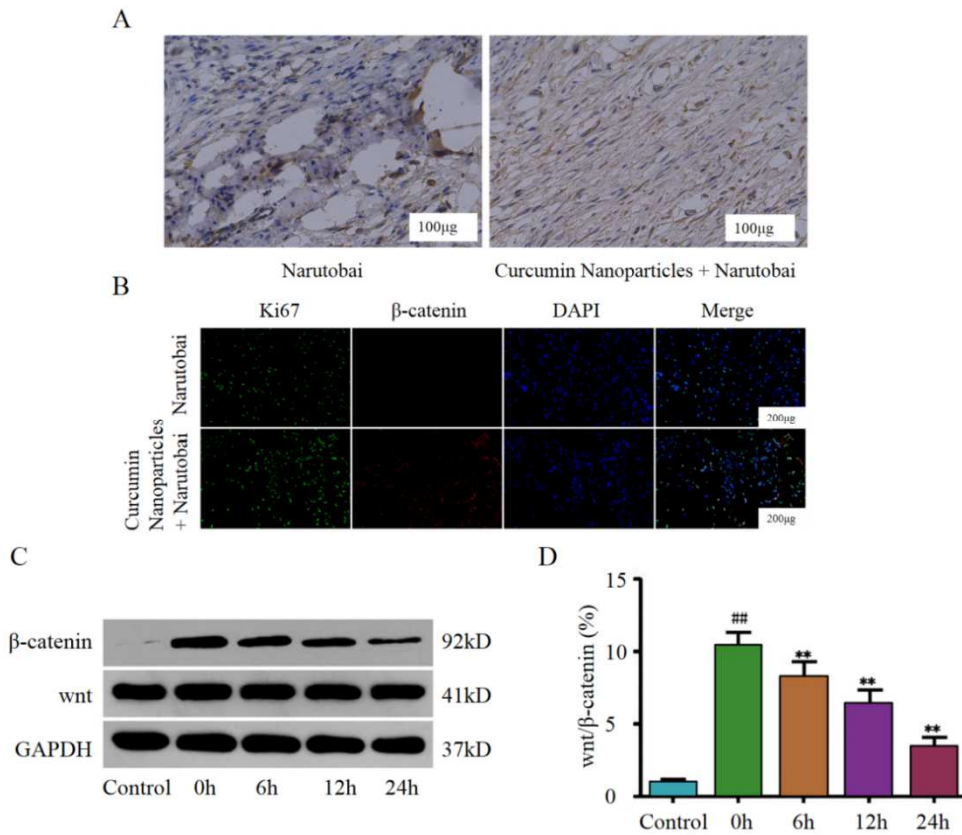


**Fig. 3:** The Wnt/β-catenin signaling pathway is the direct target gene of curcumin nanoparticles combined with narlumosbart.

(A) Protein expression levels of β-catenin in each group of cells were detected by immunohistochemistry (scale bar: 100 μm); (B) Correlation between immunofluorescence cytobiological detection and protein expression analysis (scale bar: 50 μm); (C) Key pathway protein expression was analyzed by Western blot; (D) Semi-quantitative densitometric analysis of protein bands compared to the Control group; \*\*p < 0.05, ##p < 0.01.

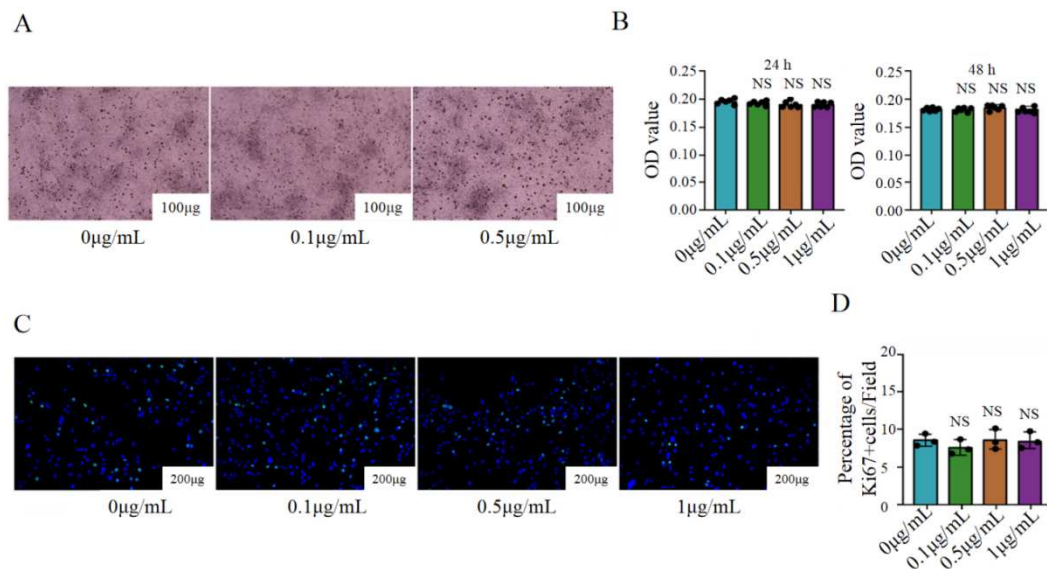


**Fig. 4:** Effect of Wnt/β-catenin on osteogenesis and maintenance of bone homeostasis.

(A) Alkaline phosphatase (ALP) activity staining results are shown (scale bar: 200 μm); (B) Effects of β-catenin on osteocyte proliferation assessed by CCK-8 assay; (C) Representative immunofluorescence images of Ki-67 staining (scale bar: 50 μm); (D) Statistical analysis of Ki-67-positive cell rate (NS: not significant, p > 0.05).

Although previous studies have suggested that curcumin inhibits the nuclear translocation of  $\beta$ -catenin, the co-administration of curcumin nanoparticles with narlumosbart in this study may influence upstream signaling by regulating other components of the Wnt/ $\beta$ -catenin pathway, such as GSK-3 $\beta$  or LRP5/6, thereby indirectly enhancing  $\beta$ -catenin expression and signaling activity. This phenomenon suggests that the combination therapy may counteract the inhibitory effect observed with curcumin monotherapy through multi-target mechanisms.

Most hormonal or drug treatments for bone degeneration also reduce bone formation. This study did not include animal experiments. Future studies will aim to validate the *in vitro* findings using animal models of bone defects, such as injecting curcumin nanoparticles + narlumosbart into wild-type mice. The *in-vitro* findings in this study demonstrated that this co-treatment effectively activates the Wnt/ $\beta$ -catenin pathway in osteoblasts and promotes their differentiation, suggesting its therapeutic promise for enhancing bone regeneration. However, the actual efficacy and safety under *in-vivo* conditions require further validation through future studies using animal models of bone defects. This study provides the first evidence of the dual regulatory role of the curcumin nanoparticle-narlumosbart combination on the Wnt/ $\beta$ -catenin pathway: while curcumin monotherapy inhibits  $\beta$ -catenin nuclear translocation, the combination paradoxically enhances both its expression and signaling activity. It is hypothesized that narlumosbart, via its high-affinity binding to RANKL, may recalibrate the signaling equilibrium in the bone microenvironment, thereby modulating the feedback mechanisms of the Wnt pathway. Future investigations should focus on how this combination regulates key pathway components such as GSK-3 $\beta$  and Axin.

In summary, curcumin nanoparticles + narlumosbart have great potential as a drug for treating bone trauma diseases. Similarly, this study also has some limitations. First, the sample size was small. Second, this study was not tested on clinical samples, so in the future, the conclusion can be verified from a clinical perspective by further expanding the sample size.

## CONCLUSION

In conclusion, the combination of curcumin nanoparticles and narlumosbart enhances  $\beta$ -catenin expression and promotes osteogenic differentiation through modulation of the Wnt/ $\beta$ -catenin signaling pathway, thereby contributing to bone homeostasis maintenance without affecting cell proliferation.

### Acknowledgment

We gratefully acknowledge the People's Hospital of Dongxihu Laboratory for providing the necessary equipment for this study.

### Authors' contributions

Heng Zhang: Conceptualization, experimental design, data collection and analysis, manuscript writing, experimental operation and data processing; Yonggang Zhao: Research supervision, manuscript revision and review, material provision and technical support. All authors have read and approved the final manuscript.

### Funding

There was no funding.

### Data availability statement

The datasets generated and/or analyzed during the current study are available from the corresponding author upon reasonable request.

### Ethical approval

The ethical approval (No.: DXH-E-20230505) was granted for the overall research project, including the planning of future animal studies. The current manuscript reports only the *in vitro* phase of this project, and no animal experiments were performed as part of this study.

### Conflict of interest

The authors declare that this research was conducted in the absence of any commercial or financial relationships that could be construed as a potential conflict of interest.

## REFERENCES

- Antoon JW, Nitzchke AM, Martin EC, Rhodes LV, Nam S, Wadsworth S, Salvo VA, Elliott S, Collins-Burow B, Nephew KP and Burow ME (2013). Inhibition of p38 mitogen-activated protein kinase alters microRNA expression and reverses epithelial-to-mesenchymal transition. *Int J Oncol*, **42**(4): 1139-1150.
- Azeem A, Talegaonkar S, Negi LM, Ahmad FJ, Khar RK and Iqbal Z (2012). Oil based nanocarrier system for transdermal delivery of ropinirole: A mechanistic, pharmacokinetic and biochemical investigation. *Int J Pharm*, **422**(1-2): 436-444.
- Chao Y, Zhang L, Zhang X, Ma C and Chen Z (2020). Expression of MiR-140 and MiR-199 in synovia and its correlation with the progression of knee osteoarthritis. *Med Sci Monit*, **26**: e918174.
- Chen S, Ye J, Chen X, Shi J, Wu W, Lin W, Lin W, Li Y, Fu H and Li S (2018). Valproic acid attenuates traumatic spinal cord injury-induced inflammation via STAT1 and NF-kappaB pathway dependent of HDAC3. *J Neuroinflammation*, **15**(1): 150.
- Collaborators GBDF (2021). Global, regional, and national burden of bone fractures in 204 countries and territories, 1990-2019: A systematic analysis from the Global Burden of Disease Study 2019. *Lancet Healthy Longev*, **2**(9): e580-e592.
- Coupaud S, McLean AN, Purcell M, Fraser MH and Allan DB (2015). Decreases in bone mineral density at cortical

- and trabecular sites in the tibia and femur during the first year of spinal cord injury. *Bone*, **74**: 69–75.
- Dai B, Qiao L, Zhang M, Cheng L, Zhang L, Geng L, Shi C, Zhang M, Sui C, Shen W, Sun Y, Chen Q, Hui D, Wang Y and Yang J (2019). lncRNA AK054386 functions as a ceRNA to sequester miR-199 and induce sustained endoplasmic reticulum stress in hepatic reperfusion injury. *Oxid Med Cell Longev*, **2019**: 8189079.
- Fan J, Schiemer T, Vaska A, Jahed V and Klavins K (2024). Cell via cell viability assay changes cellular metabolic characteristics by intervening with glycolysis and pentose phosphate pathway. *Chem Res Toxicol*, **37**(2): 208-211.
- Li SY, Zhou HL, Hu C, Yang JB, Ye JF, Zhou YX, Li ZG, Chen LL and Zhou QS (2021). Total flavonoids of rhizoma drynariae promotes differentiation of osteoblasts and growth of bone graft in induced membrane partly by activating Wnt/ $\beta$ -catenin signaling pathway. *Front Pharmacol*, **12**: 1-14.
- Liu Z, Yao X, Jiang W, Li W, Zhu S, Liao C, Zou L, Ding R and Chen J (2020). Advanced oxidation protein products induce microglia-mediated neuroinflammation via MAPKs-NF-kappaB signaling pathway and pyroptosis after secondary spinal cord injury. *J Neuroinflammation*, **17**(1): 90.
- Lv YJ, Wang P, Huang R, Liang XX, Wang P, Tan JB, Chen ZH, Dun ZJ, Wang J, Jiang Q, Wu SX, Ling HT, Li ZX and Yang XF (2017). Cadmium exposure and osteoporosis: A population-based study and benchmark dose estimation in southern China. *J Bone Miner Res*, **32**(10): 1990-2000.
- Mai YX, Li ZP, Pang FX, Zhou ST, Li N, Wang YY and Zhang JF (2024). Aucubin promotes osteogenic differentiation and facilitates bone formation through the lncRNA-H19 driven Wnt/ $\beta$ -catenin signaling regulatory axis. *Stem Cells Int*, **2024**: 5388064.
- Mitchell SAT, Majuta LA and Mantyh PW (2018). New insights in understanding and treating bone fracture pain. *Curr Osteoporos Rep*, **16**(4): 325-332.
- Niu YF, Chen L and Wu TF (2023). Recent advances in bioengineering bone revascularization based on composite materials comprising hydroxyapatite. *Int J Mol Sci*, **24**(15): 12492.
- Richbourg HA, Hu DP, Xu Y, Barczak AJ and Marcucio RS (2020). miR-199 family contributes to regulation of sonic hedgehog expression during craniofacial development. *Dev Dyn*, **249**(9): 1062-1076.
- Rishabh K, Khadilkar S, Kumar A, Kalra I, Kumar AP and Kunnumakkara AB (2021). MicroRNAs as modulators of oral tumorigenesis-a focused review. *Int J Mol Sci*, **22**(5): 2561.
- Seitz S, Priemel M, von Domarus C, Beil FT, Barvencik F, Amling M and Rueger JM (2008). The second most common bone disease: A review on paget's disease of bone. *Eur J Trauma Emerg Surg*, **34**(6): 549-553.
- Shi JC, Zhang BQ, Wu ZQ, Zhang YH, Gupta A, Wang XD, Wang JY, Pan LS, Xiao M, Zhang SJ and Wang L (2024). Peripheral nerve-derived Sema3A promotes osteogenic differentiation of mesenchymal stem cells through the Wnt/ $\beta$ -catenin/Nrp1 positive feedback loop. *J Cell Mol Med*, **28**(8): 1-15.
- Tomlinson RE, Li Z, Li Z, Minichiello L, Riddle RC, Venkatesan A and Clemens TL (2017). NGF-TrkA signaling in sensory nerves is required for skeletal adaptation to mechanical loads in mice. *Proc Natl Acad Sci USA*, **114**(18): E3632-E3641.
- Wan QQ, Qin WP, Ma YX, Shen MJ, Li J, Zhang ZB, Chen JH, Tay FR, Niu LN and Jiao K (2021). Crosstalk between bone and nerves within bone. *Adv Sci*, **8**(7): 2-24.
- Wang XD, Li SY, Zhang SJ, Gupta A, Zhang CP and Wang L (2020). The neural system regulates bone homeostasis via mesenchymal stem cells: A translational approach. *Theranostics*, **10**(11): 4839-4850.
- Wei DY, Shen BH, Wang WX, Zhou YJ, Yang XD, Lu GJ, Yang JB and Shao YB (2019). MicroRNA-199a-5p functions as a tumor suppressor in oral squamous cell carcinoma via targeting the IKK $\beta$ /NF- $\kappa$ B signaling pathway. *Int J Mol Med*, **43**(4): 1585-1596.
- Wu L, Wei QZ, Lv YJ, Xue JC, Zhang B, Sun Q, Xiao T, Huang R, Wang P, Dai XY, Xia HB, Li JJ, Yang XF and Liu QZ (2019). Wnt/ $\beta$ -catenin pathway is involved in cadmium-induced inhibition of osteoblast differentiation of bone marrow mesenchymal stem cells. *Int J Mol Sci*, **20**(6): 1519.
- Zhu JH, Liao YP, Li FS, Hu Y, Li Q, Ma Y, Wang H, Zhou Y, He BC and Su YX (2018). Wnt11 promotes BMP9-induced osteogenic differentiation through BMPs/Smads and p38 MAPK in mesenchymal stem cells. *J Cell Biochem*, **119**(11): 9462-9473.
- Zhu Y, Luo L, Zhang M, Song X, Wang P, Zhang H, Zhang J and Liu D (2023). Xuanfei Baidu formula attenuates LPS-induced acute lung injury by inhibiting the NF-kappaB signaling pathway. *J Ethnopharmacol*, **301**:115833.
- Zhuang H, Ren X, Jiang F and Zhou P (2023). Indole-3-propionic acid alleviates chondrocytes inflammation and osteoarthritis via the AhR/NF-kappaB axis. *Mol Med*, **29**(1): 17.